Measurement of Atmospheric Production Depths of muons with the Pierre Auger Observatory

D. GARCÍA-GÁMEZ[1] FOR THE PIERRE AUGER COLLABORATION[2]
[1]*Laboratoire de l'Accélérateur linéaire (LAL), Université Paris 11, CNRS-IN2P3, Orsay, France*
[2]*Observatorio Pierre Auger, Av. San Martin Norte 304, 5613 Malargüe, Argentina*
(Full author list: http://www.auger.org/archive/authors_2011_05.html)
auger_spokespersons@fnal.gov

Abstract: The surface detector array of the Pierre Auger Observatory provides information about the longitudinal development of the hadronic component of extensive air showers in an indirect way. In this contribution we show that it is possible to reconstruct the Muon Production Depth distribution (MPD) using the FADC traces of surface detectors far from the shower core. We characterize the goodness of this reconstruction for zenith angles around 60° and different energies of the primary particle. From the MPDs we define $X^{\mu}_{\max}$ as the depth, along the shower axis, where the number of muons produced reaches a maximum. We explore the potentiality of $X^{\mu}_{\max}$ as a sensitive parameter to determine the mass composition of cosmic rays.

Keywords: Muon Production Depth distributions, Pierre Auger Observatory

1 Introduction

The Pierre Auger Observatory was conceived to study the properties of Ultra-High Energy Cosmic Rays (UHECR). It is a hybrid detector that combines both surface and fluorescence detectors at the same site [1]. The origin and chemical composition of UHECR are still an enigma. Currently, the most sensitive parameter to analyse mass composition is the depth of the shower maximum, $X_{\max}$, see e.g. [2, 3], measured by the fluorescence detector (FD) [4]. The fluorescence detector operates only on clear, moonless nights, so its duty cycle is small (about 13 %). On the other hand, the surface detector array (SD) [5] has a duty cycle close to 100 %. This increase in statistics makes any SD-based observable of great interest to study the composition of UHECR.

In an extensive air shower (EAS) muons are mainly produced by the decay of pions and kaons. Their production points are constrained to a region very close to the shower axis, of the order of tens of meters [6]. Muons can be taken as travelling along straight lines to ground, due to the lesser importance of bremsstrahlung and multiple scattering effects compared to other geometrical and kinematical factors. In [6, 7] these features are exploited to build a model for obtaining the muon production depth (MPD) along the shower axis. The MPDs are calculated from the muon time structure at ground. These times are given along with the times of the other particles reaching ground by the FADCs of the SD. In this work we show that MPDs provide a physical observable that can be used as a sensitive parameter to study the chemical composition of cosmic rays [8].

2 MPD reconstruction

Starting from the time signals that muons produce in the surface detectors, the model discussed in [6, 7] derives from geometrical arguments the distribution of muon production distance, z:

$$z = \frac{1}{2}\left(\frac{r^2}{ct_g} - ct_g\right) + \Delta \quad (1)$$

where r is the distance from the point at ground to the shower axis, Δ is the distance from the same point to the shower plane and t_g (*geometrical delay*) is the time delay with respect to the shower front plane. The shower front plane is defined as the plane perpendicular to the shower axis and moving at the speed of light, c, in the direction of the shower axis. It contains the first interaction point and also the core hitting ground. This calculation assumes that muons travel at the speed of light. If we account for their finite energy E, the total time delay would be $ct = ct_g + ct_{\epsilon}(E)$. This extra contribution is dominant at short distances to the core, where the geometrical time delay is very small. At large distances ($r > 600$ m) the *kinematic delay*, t_{ϵ}, acts as a correction (typically below 20%). It must be subtracted from the measured time delay prior to the conversion into z, as described in [6, 7].

Equation 1 gives a mapping between the production distance z and the *geometrical delay* t_g for each point at

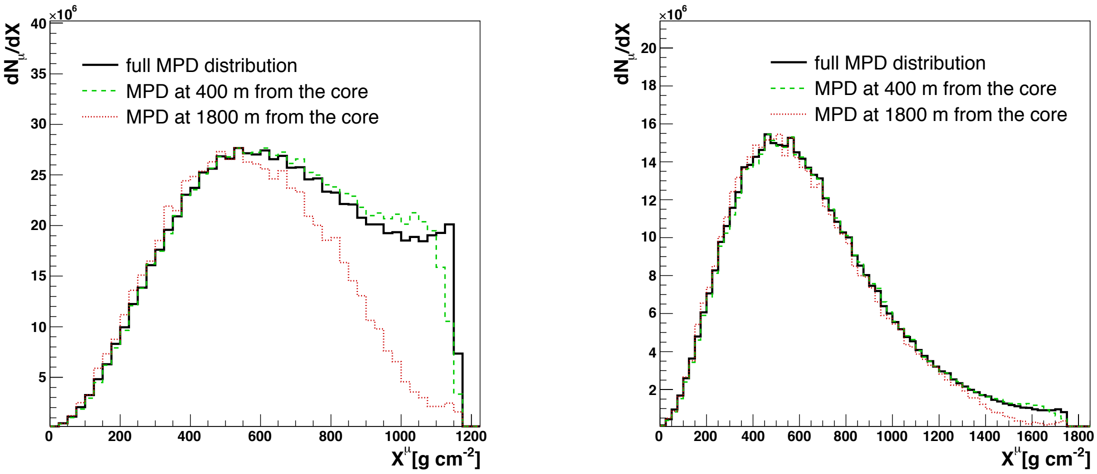

Figure 1: Muon production depth distributions (MPDs) extracted from an iron shower of 10^{19} eV simulated with AIRES [10] at two different zenith angles: 41° (left) and 60° (right). The MPD dependence with the distance to the core is shown.

ground. The production distance can be easily related to the total amount of traversed matter X^μ using

$$X^\mu = \int_z^\infty \rho(z')dz' \tag{2}$$

where ρ is the atmosphere density. This X^μ distribution is referred to as MPD. The shape of the MPD contains relevant information about the development of the hadronic cascade and the first interaction point. To extract valuable physics insight from the MPD we perform a fit. It was found that a Gaisser-Hillas function [9] can describe the shape of the MPD well. The fit with this function provides the maximum of the distribution, $X^\mu_{\max}$. We interpret $X^\mu_{\max}$ as the point where the production of muons reaches the maximum along the cascade development. As shown in the following sections, this new observable can be used for composition studies.

The MPD is populated with the surviving muons reaching ground, so its shape depends on the zenith angle. Figure 1 displays MPDs directly extracted from AIRES simulations [10] at different zenith angles and at different distances from the core, r. For angles of about 40° and lower, the shape of the MPD and the position of its maximum show a strong r dependence. However, at zenith angles of around 60° and above, where the showers develop very high in the atmosphere, the differences between the MPD at different distances to the core become small. Thus, for those showers we can add in the same histogram the X^μ values given by the time signals from the different surface detectors. The addition of the signals from the different surface detectors contributing to the MPD at small zenith angles would demand the introduction of a correction factor that transforms all those signals to the one expected at a reference r (see [6, 7] for a thorough discussion about this correction). At larger zenith angles the distortion due to the detector time resolution becomes larger. The above reasons lead us to select the data with measured zenith angles between 55° and 65° for our analysis.

2.1 Detector effects

The precision of the method is limited so far by the detector capabilities. The total uncertainty of the MPD maximum, $\delta X^\mu_{\max}$, decreases as the square root of the number of muons N_μ, and decreases quadratically with the distance to the core r. This last uncertainty is linked to each single time bin entry of the FADC traces. To keep the distortions on the reconstructed MPD small, only detectors far from the core can be used. The cut in r diminishes the efficiency of the reconstruction, as the number of muons contributing to the MPD is reduced. Hence a r_{cut} value must be carefully chosen in order to guarantee good reconstruction efficiencies, avoiding at the same time a bias on the mass of the primary.

Furthermore, signals collected by the water Cherenkov detectors are the sum of the electromagnetic (EM) and muonic components. Both exhibit a different arrival time behavior. As a consequence, a cut on signal threshold, rejecting all time bins with signal below a certain value, might help diminishing the contribution of the EM contamination. The so called EM halo, coming from the decay of muons in flight, is harder to suppress. But this component follows closer the time distribution of their parent muons, thus it does not hamper our analysis.

2.2 Reconstruction cuts

To study and select the cuts needed for a good MPD reconstruction and an accurate $X^\mu_{\max}$ determination we have used Monte Carlo simulations. The selection of cuts must be a trade off between the resolution of the reconstructed MPD and the number of muons being accepted into such

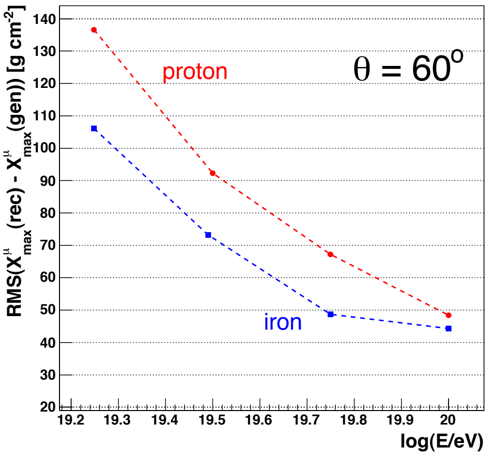

Figure 2: Energy evolution of the resolution we obtain, on an event by event basis, when we reconstruct $X^{\mu}_{\max}$ for showers generated with AIRES and QGSJETII [11].

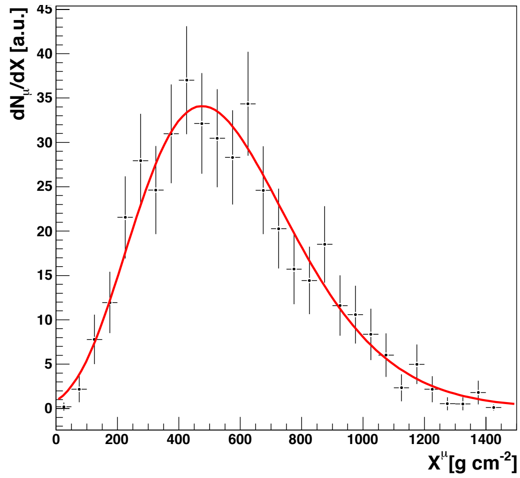

Figure 3: Real reconstructed MPD, θ = (59.05 $\pm$ 0.07) ° and E = (94 $\pm$ 3) EeV, with its fit to a Gaisser-Hillas function.

reconstruction. The chosen r_{cut} is energy independent. This implies that any difference in resolution that we find for different energies will be mainly a consequence of the different amount of muons detected at ground. In our analysis, we consider only those detectors whose distance to the shower core is larger than 1800 m. To reduce residual EM contamination and potential baseline fluctuations we have applied a mild cut on the threshold of the FADC signals used to build the MPD. We have discarded FADC bins where the signal is below 0.3 VEM. Finally, the MPD is reconstructed adding those detectors whose total recorded signal is above 3 VEM. This requirement is set to avoid, in real data, the contribution of detectors (usually far away from the core) having a signal dominated by accidental particles.

This set of cuts has a high muon selection efficiency. Regardless of the energy of the primary and its composition, muon fractions above 85% are always obtained. This guarantees an EM contamination low enough to obtain an accurate value of $X^{\mu}_{\max}$.

2.3 Selection cuts

To optimize the quality of our reconstructed profiles we apply the following cuts:

- **Trigger cut**: All events must fulfill the T5 trigger condition [5].
- **Energy cut**: Since the number of muons is energy dependent, $N_{\mu} \propto E^{\alpha}/r^{\beta}$, we have observed that in events with energies below 20 EeV the population of the MPD is very small, giving a very poor determination of the $X^{\mu}_{\max}$ observable. Therefore we restrict our analysis to events with energy larger than 20 EeV.
- **Fit quality**: Only events with a good MPD fit (χ^2/ndf < 2.5) to a Gaisser-Hillas function are accepted.
- **Shape cut**: The reduced χ^2 of a straight line and a Gaisser-Hillas fit must satisfy χ^2_{GH}/ndf $<$ $2\chi^2_{line}$/ndf.
- **Curvature**: When the fitted radius of curvature of the shower front, R, is very large we observe an underestimation of the reconstructed $X^{\mu}_{\max}$. So only events with $R <$ 29000 m are included in our analysis.

The overall event selection efficiencies are high ($>$ 80%) and the difference between iron and proton is small for the whole range of considered energies (see Table 1). Our cuts do not introduce any appreciable composition bias. We finally note that for the set of surviving events, the bias in the $X^{\mu}_{\max}$ reconstruction is between $\pm$ 10 g cm^{-2}, regardless of the initial energy or the chemical composition of the primary. The resolution ranges from about 120 g cm^{-2} at the lower energies to less than 50 g cm^{-2} at the highest energy (see Figure 2).

We note that the predictions of $X^{\mu}_{\max}$ from different hadronic models (such as those shown in Figure 4) would not be affected if a discrepancy between a model and data [12] is limited to the *total* number of muons. However, differences in the muon energy and spatial distribution would modify the predictions.

3 Application to real data

Our analysis makes use of the data collected between January 2004 and December 2010. Our initial sample of events

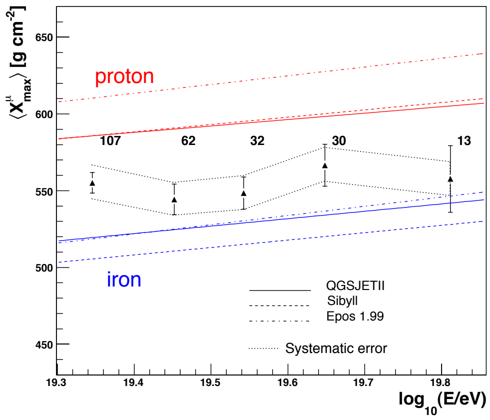

Figure 4: $\langle X^{\mu}_{\max} \rangle$ as a function of the energy. The number of real data events in each energy bin is indicated. The predictions for proton and iron following different hadronic models are shown as well.

Table 1: Selection efficiencies for proton and iron QGSJETII Monte Carlo showers as a function of energy.

$\log_{10}$(E/eV)	ε_p (%)	ε_{Fe} (%)	$\lvert\varepsilon_p - \varepsilon_{Fe}\rvert$ (%)
19.25	82	87	6
19.50	84	86	2
19.75	85	82	3
20.00	95	97	2

with zenith angle $\theta \in [55°, 65°]$ and a reconstructed energy bigger than 20 EeV consists of 417 events. The overall selection efficiency amounts to 58%, which translates into 244 surviving events. The difference between the efficiencies shown in Table 1 and the selection efficiency in real data is due to the T5 cut [5]. This cut has an efficiency of about 72% for data, while all our Monte Carlo showers are generated as T5 events. We compute MPDs on an event by event basis. Figure 3 shows the reconstructed MPD for one of our most energetic events. The evolution of the $\langle X^{\mu}_{\max} \rangle$ observable as a function of energy is shown in Figure 4. The selected data has been grouped into five bins of energy. Each bin has a width of 0.1 in $\log_{10}$(E/eV), except the last one which contains all the events with energy larger than $\log_{10}$(E/eV)=19.7. The error bars correspond to the ratio between the RMS of the distributions of $X^{\mu}_{\max}$ and the square root of the number of entries. If compared to air shower predictions using standard interaction models, our measurement is compatible with a mixed composition.

Table 2 lists the most relevant sources contributing to the systematic uncertainty. The uncertainties on the MPD reconstruction and event selection translate into a systematic uncertainty on $\langle X^{\mu}_{\max} \rangle$ of 11 g cm^{-2}.

4 Conclusions

We have shown that it is possible to reconstruct the muon production depth distribution using the FADC traces of the SD detectors far from the core. From the MPDs we define a new observable $X^{\mu}_{\max}$. It measures the depth along the shower axis where the number of produced muons reaches a maximum. We have characterized the applicability of this observable and analysed its resolution for zenith angles $\sim$ 60° and different shower energies. We have demonstrated, for the first time, that $X^{\mu}_{\max}$ is a parameter sensitive to the mass composition of UHECR. The result of this study is in agreement with all previous Auger results [13] obtained with other completely independent methods.

Table 2: Evaluation of the main sources of systematic uncertainties.

Source	Sys. Uncertainty (g cm^{-2})
Reconstruction bias	9.8
Core position	4.8
EM contamination	1.5
χ^2 cut	0.2
Selection efficiency	1
Total	11

References

[1] J. Abraham *et al.* , Nucl. Instr. and Meth. A, 2004, **523**(1-2): 50-95

[2] J. Abraham *et al.* , Phys. Rev. Lett., 2010, **104** (9): 1-7

[3] R. U. Abbasi *et al.* , Phys. Rev. Lett., 2010, **104**(16): 161101

[4] J. Abraham *et al.* , Nucl. Instr. and Meth. A, 2010, **620**(2-3): 227-251

[5] J. Abraham *et al.* , Nucl. Instr. and Meth. A, 2010, **613**(1): 29-39

[6] L. Cazon, R.A. Vazquez, A.A. Watson, E. Zas, Astropart. Phys., 2004, **21**(1): 71-86

[7] L. Cazon, R.A. Vazquez, E. Zas, Astropart. Phys., 2005, **23**(4): 393-409

[8] D. Garcia-Gamez, Muon Arrival Time distributions and its relationship to the mass composition of Ultra High Energy Cosmic Rays: An application to the Pierre Auger Observatory, Universidad de Granada, PhD Thesis, 2010

[9] T. K. Gaisser and A. M. Hillas, Proceedings, 15th International Cosmic Ray Conference, **8** , 13-26

[10] S. Sciutto, Proceedings, 27th International Cosmic Ray Conference, 2001, arXiv: astro-ph/0106044

[11] S. Ostapchenko, AIP Conference Proceeding, 2007, **928**, 118-125

[12] J. Allen, for the Pierre Auger Collaboration, paper 0703, these proceedings

[13] D. Garcia-Pinto, for the Pierre Auger Collaboration, paper 0709, these proceedings